Scientia Iranica, Vol. 10, No. 1, pp 13–22

SCIENTIA
IRANICA

Thermomechanical Shocks in Composite Cylindrical Shells: A Coupled Thermoelastic Finite Element Analysis

B. Shiari[1], M.R. Eslami* and M. Shaker[1]

In this paper, the coupled dynamic thermoelastic response of multilayer composite cylindrical shells to thermomechanical shocks is examined in the present article. An explicit and integrated finite element method is employed to solve the associated coupled thermoelastic equations. The classical linear thermoelastic theory is considered for the laminated composite shell, based on the second order shell theory, including normal stress and strain, as well as transverse shear and rotary inertia. Composite cylindrical shells under thermal and mechanical shock loads are examined and the effect of thermomechanical coupling, layer stacking sequence and normal stress are examined.

INTRODUCTION

In aerospace applications, cases of instant thermomechanical loading of structures are abundant. It is well known that under the circumstances where a structure is exposed to a high rate of thermal loading, the induced displacement and temperature fields cannot be analyzed independently. In these cases, the thermomechanical coupling exists and must be taken into account in the analysis. The analytical approaches to solution of the structural members subjected to such loading conditions are mathematically complicated and are limited to the problems of infinite-space and half-space.

McQuillen and Brull worked out one of the earliest numerical investigations of coupled thermoelasticity of thin shells using the traditional Galerkin method [1]. They considered the first order shell theory, based on the Love assumptions, and essentially ignored normal stress, transverse shear stress and rotary inertia, but assumed a nonlinear temperature distribution across the shell thickness. They concluded that the difference between the coupled and uncoupled solutions are about one percent. Li et al. [2] and Eslami and Vahedi [3] used the Galerkin finite element method and applied it to the coupled thermoelasticity of thick cylinders and spheres. Thin cylindrical shells under thermal shock are studied by Takazono [4] where the uncoupled equations of a shell are considered and viscoplasticity of the shell is discussed. The coupled thermoelasticity of thin cylindrical shells is studied by Eslami et al. [5], where the first order shell theory, based on the Love assumption, is used and the proper Galerkin finite element formulation is presented. Since the analysis is performed for long thin cylindrical shells, axial displacement is ignored and only lateral shell displacement is considered in the analysis. Wang et al. [6] studied the behavior of multilayered cylinders subjected to a high rate of thermal heating, considering thermomechanical coupling, but the inertia effect neglecting. Since most of the advanced composite materials show anisotropic behavior, the concept of a unique thermomechanical coupling term is dispensed with making classical analytical solutions virtually impossible. Consequently, the numerical methods turn out to be the only option. The coupled thermoelasticity of general shells of the revolution of isotropic and homogeneous material, based on the Flugge second order shell theory, is discussed by Eslami et al. [7,8]. In this paper, the effects of normal stress, transverse shear stress and rotary inertia are considered. The paper is mainly based on the classical coupled thermoelasticity assumption, although the second sound effect, based on the Lord-Shulman theory, is briefly discussed.

In this paper, a multilayer orthotropic composite cylindrical shell under thermal and mechanical shocks,

1. *Department of Mechanical Engineering, Amir Kabir University of Technology, Tehran, I.R. Iran.*
*. *Corresponding Author, Department of Mechanical Engineering, Amir Kabir University of Technology, Tehran, I.R. Iran.*

resulting in a coupled thermoelastic field, is considered. The full stress-strain relations of the three-dimensional theory of elasticity is considered and the Flugge second order shell theory, which is the most complete compared to other classical second order theories, is employed to formulate the coupled thermoelasticity of shells of revolution. The results are obtained with formulation, where normal stress is considered and the effect of normal stress in composite shell response is evaluated. Furthermore, the effect of coupling and layer stacking is studied and the results are compared for coupled and uncoupled models.

DERIVATIONS

Consider a thin cylindrical shell of thickness h and mean radius R with the principal coordinate system (x, θ, z), as shown in Figure 1, where $z-$coordinate measures from the shell middle plane. The shell is assumed to be under thermomechanical loadings, where the load is assumed to be axisymmetric and uniformly distributed along the $x-$axis. To write the shell governing equations, one starts from the assumption of displacement distribution across the shell thickness. The basic assumption to consider normal stress and strain in shell equations, requires relating the displacement components along the principal orthogonal curvilinear coordinates of the shell, namely U, V and W, to the displacement components on the middle plane, as given by the following relations [9]:

$$U(x,\theta,z) = u_0(x,\theta) + z\psi_x(x,\theta),$$

$$V(x,\theta,z) = v_0(x,\theta) + z\psi_\theta(x,\theta),$$

$$W(x,\theta,z) = w_0(x,\theta) + z\psi_z(x,\theta) + \frac{z^2}{2}\phi_z(x,\theta), \qquad (1)$$

where (x, θ, z) are the principal orthogonal curvilinear coordinates of the shell, u_0, v_0 and w_0 are the middle plane displacements, ψ_x and ψ_θ are rotations of the tangent line to the middle plane along x and θ axes, respectively, and ψ_z and ϕ_z are related to the non-zero transverse normal strains.

The strain-displacement relations for the second order shell theory are:

$$\epsilon_x = u_{0,x} + z\psi_{x,x},$$

$$\epsilon_\theta = \frac{1}{1+\frac{z}{R}}\left[\frac{1}{R}(v_{0,\theta} + w_0 + z\psi_{\theta,\theta} + z\psi_z + \frac{1}{2}z^2\phi_z)\right],$$

$$\epsilon_z = \psi_z + z\phi_z,$$

$$\gamma_{x\theta} = v_{0,x} + z\psi_{\theta,x} + \frac{1}{1+\frac{z}{R}}[\frac{1}{R}(u_{0,\theta} + z\psi_{x,\theta})],$$

$$\gamma_{xz} = w_{0,x} + \psi_x + z\psi_{z,x} + \frac{1}{2}z^2\phi_{z,x},$$

$$\gamma_{\theta z} = \frac{1}{1+\frac{z}{R}}[\frac{1}{R}(w_{0,\theta} - v_0 + R\psi_\theta + z\psi_{z,\theta} + \frac{1}{2}z^2\phi_{z,\theta})], \qquad (2)$$

where ϵ's are the normal strains and γ_{ij} are the shear strains. The sign $(,)$ in the subscript indicates partial derivative. These relations are obtained, based on the Flugge second order shell theory, where the term z/R is retained in the equations compared to the unity.

The forces and moments resultants, based on the second order shell theory, are defined as:

$$< N_x, A, N_{x\theta}, Q_x > = \int_{-h}^{+h} (\sigma_x, \sigma_z, \tau_{x\theta}, \tau_{xz})(1 + \frac{z}{R})dz,$$

$$< N_\theta, N_{\theta x}, Q_\theta > = \int_{-h}^{+h} (\sigma_\theta, \tau_{x\theta}, \tau_{\theta z})dz,$$

$$< M_x, B, M_{x\theta}, S_x > = \int_{-h}^{+h} (\sigma_x, \sigma_z, \tau_{x\theta}, \tau_{xz})(1 + \frac{z}{R})zdz,$$

$$< M_\theta, M_{\theta x}, S_\theta > = \int_{-h}^{+h} (\sigma_\theta, \tau_{x\theta}, \tau_{\theta z})zdz,$$

$$P_\theta = \frac{1}{2}\int_{-h}^{+h} \sigma_\theta z^2 dz,$$

$$T_x = \int_{-h}^{+h} \tau_{xz}(1 + \frac{z}{R})z^2 dz,$$

$$T_\theta = \int_{-h}^{+h} \tau_{\theta z}(1 + \frac{z}{R})z^2 dz, \qquad (3)$$

where N_{ij} and M_{ij} are the forces and moments per unit length of shell, Q_i is the transverse shear force and A, B, S_i, P_θ, and T_i are just some shell generalized forces as defined in Equations 3 [9].

The equations of motions may be obtained using the Hamilton's variational principle [9]. For this general case, where normal stress and strain are included in the governing equations, Hamilton principle yields

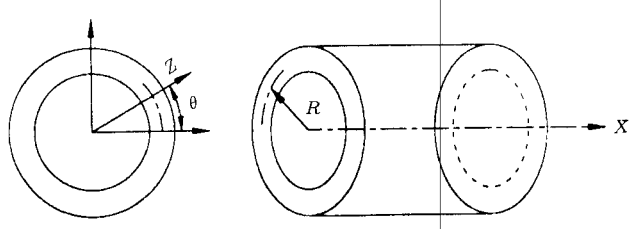

Figure 1. Shell coordinates.

the following equilibrium equations:

$$
\begin{aligned}
&N_{x,x}+\frac{N_{\theta x,\theta}}{R}=I_1\ddot{u}_0+I_2\ddot{\psi}_x,\\
&\frac{N_{\theta,\theta}}{R}+N_{x\theta,x}+\frac{Q_\theta}{R}=I_1\ddot{v}_0+I_2\ddot{\psi}_\theta,\\
&-\frac{N_\theta}{R}+Q_{x,x}+\frac{Q_{\theta,\theta}}{R}-Rq_z=I_1\ddot{w}_0+I_2\ddot{\psi}_z+\frac{I_3}{2}\ddot{\phi}_z,\\
&M_{x,x}+\frac{M_{\theta x,\theta}}{R}-Q_x=I_2\ddot{u}_0+I_3\ddot{\psi}_x,\\
&\frac{M_{\theta,\theta}}{R}+M_{x\theta,x}-Q_\theta=I_2\ddot{v}_0+I_3\ddot{\psi}_\theta,\\
&-\frac{M_\theta}{R}+S_{x,x}-A+\frac{S_{\theta,\theta}}{R}=I_2\ddot{w}_0+2I_3\ddot{\psi}_z+\frac{I_4}{2}\ddot{\phi}_z,\\
&-\frac{P_\theta}{R}-B+T_{x,x}-\frac{T_{\theta,\theta}}{R}-\frac{h^2}{8}q_z=\frac{I_3}{2}\ddot{w}_0+\frac{I_4}{2}\ddot{\psi}_z+\frac{I_4}{4}\ddot{\phi}_z,
\end{aligned}
\tag{4}
$$

where the moments of inertia, I_n, are defined as:

$$
I_n=\int_{-h}^{h}\rho z^{(n-1)}(1+\frac{z}{R})dz\quad n=1,2,..,5. \tag{5}
$$

Here, q_z and m_z are the components of external forces and moments acting on the middle plane of the shell. These forces and moments are related to the external applied forces q_z^+ and q_z^- as [9]:

$$
\begin{aligned}
q_z&=q_z^+(1+\frac{z}{R})+q_z^-(1-\frac{z}{R}),\\
m_z&=\frac{z}{2}[q_z^+(1+\frac{z}{R})-q_z^-(1-\frac{z}{R})].
\end{aligned}
\tag{6}
$$

The stress-strain relation for the kth orthotropic layer, bounded by surfaces at $z=h_{k-1}$ and $z=h_k$, are given by:

$$
\begin{bmatrix}\sigma_x\\ \sigma_\theta\\ \sigma_z\\ \tau_{\theta z}\\ \tau_{xz}\\ \tau_{x\theta}\end{bmatrix}_k=\begin{bmatrix}\bar{Q}_{11}&\bar{Q}_{12}&\bar{Q}_{13}&0&0&\bar{Q}_{16}\\ \bar{Q}_{21}&\bar{Q}_{22}&\bar{Q}_{23}&0&0&\bar{Q}_{26}\\ \bar{Q}_{31}&\bar{Q}_{32}&\bar{Q}_{33}&0&0&\bar{Q}_{36}\\ 0&0&0&\bar{Q}_{44}&\bar{Q}_{45}&0\\ 0&0&0&\bar{Q}_{54}&\bar{Q}_{55}&0\\ \bar{Q}_{61}&\bar{Q}_{62}&\bar{Q}_{63}&0&0&\bar{Q}_{16}\end{bmatrix}_k\begin{bmatrix}\epsilon_x\\ \epsilon_\theta\\ \epsilon_z\\ \gamma_{\theta z}\\ \gamma_{xz}\\ \gamma_{x\theta}\end{bmatrix}_k
$$

$$
-\begin{bmatrix}\bar{\beta}_x\\ \bar{\beta}_\theta\\ \bar{\beta}_z\\ 0\\ 0\\ \bar{\beta}_{x\theta}\end{bmatrix}_k[T]_k, \tag{7}
$$

where $[\bar{Q}_{ij}]_k$ and $[\bar{\beta}_i]_k$ are the stiffness and thermoelastic matrixes, respectively [10].

The lamination constitutive relations are given by matrix $(a-1)$ in Appendix. Substituting the element of matrix $(a-1)$ into the motion Equation 4, results in seven Navier type equations for cylindrical shells, in terms of the displacement components u_0, v_0, w_0, rotations ψ_θ, ψ_x and the transverse strains ψ_z, ϕ_z.

ENERGY EQUATION

The thermoelastic coupled heat conduction equation for the anisotropic media may be derived from the energy conservation relation, based on the first law of thermodynamics and the definition of specific entropy in the form:

$$
k_{ij}T_{,ij}-[c_\nu\rho\dot{T}+T_a\beta_{ij}\dot{\epsilon}_{ij}]=0, \tag{8}
$$

where the constants in Equation 8 are defined in the nomenclature.

One may assume a linear temperature distribution across the shell thickness as [7,10]:

$$
T(x,\theta,z,t)=T_0(x,\theta,t)+zT_1(x,\theta,t), \tag{9}
$$

where T_0 and T_1 are unknown functions to be obtained through the coupled system of equations. Following McQuillen and Brull [1], the traditional Galerkin method is used to derive two independent heat conduction equations of the shell of revolution from Equation 8, by averaging it across the shell thickness z. Due to the assumption of linear temperature variation across the shell thickness, as given by Equation 9, two unknowns T_0 and T_1 appear in the energy equation. For multilayer composite cylindrical shells under axisymmetric thermal shock, uniformly distributed along the $x-$axis, the energy Equation 8 in terms of the displacement components, reduces to:

$$
\begin{aligned}
\text{Residual}=&\rho c\dot{T}+T_a[\beta_{xx}\dot{U}_{,x}++\frac{\beta_{\theta\theta}}{R+z}\dot{W}\\
&+\beta_{zz}\dot{W}_{,z}+\beta_{x\theta}\dot{V}_{,x}]-k_{xx}\frac{\partial^2T}{\partial x^2}\\
&-k_{zz}(\frac{\partial^2T}{\partial z^2}+\frac{1}{R+z}\frac{\partial T}{\partial z}).
\end{aligned}
\tag{10}
$$

The following two integrals of the energy equation provide two independent energy equations for two independent functions, T_0 and T_1, as follows [1,7]:

$$
\begin{aligned}
&\int_z(\text{Residual}).(1).dz=0,\\
&R_c^{(1)}\dot{T}_0+R_c^{(2)}\dot{T}_1+R_x^{(1)}\dot{u}_{0,x}+R_x^{(2)}\dot{\psi}_{x,x}+R_{\theta x}^{(1)}\dot{\psi}_{\theta,x}\\
&+R_{\theta x}^{(1)}\dot{v}_{0,x}+R_z^{(2)}\dot{\psi}_z+R_x^{(2)}\dot{\phi}_z+\frac{1}{R}R_\theta^{(1)}\dot{w}_0\\
&+\frac{1}{R}R_\theta^{(2)}\dot{\psi}_z+\frac{1}{2R}R_\theta^{(3)}\dot{\phi}_z+R_{kx}^{(1)}T_{0,xx}\\
&+R_{kx}^{(2)}T_{1,xx}-\frac{1}{R}R_{kz}^{(1)}T_1-(h_i-h_o)T_o\\
&+h(h_i-h_o)T_1+[h_iT_i(t)-h_oT_\infty]=0,
\end{aligned}
\tag{11}
$$

$$\int_z (\text{Residual}).(z).dz = 0,$$

$$R_c^{(2)}\dot{T}_0 + R_c^{(3)}\dot{T}_1 + R_x^{(2)}\dot{u}_{0,x} + R_x^{(3)}\dot{\psi}_{x,x} + R_{\theta x}^{(2)}\dot{\psi}_{\theta,x} + R_{\theta x}^{(2)}\dot{v}_{0,x} + R_z^{(2)}\dot{\psi}_z + R_x^{(3)}\dot{\phi}_z + \frac{1}{R}R_\theta^{(2)}\dot{w}_0 + \frac{1}{R}R_\theta^{(3)}\dot{\psi}_z + \frac{1}{2R}R_\theta^{(4)}\dot{\phi}_z + R_{kx}^{(2)}T_{0,xx} + R_{kx}^{(3)}T_{1,xx} - \frac{1}{R}R_{kz}^{(2)}T_1 - h[(h_i - h_o)T_o - (h_i - h_o)T_1 - (h_i T_i(t) - h_o T_\infty)] = 0 \qquad (12)$$

where:

$$R_{kz}^{(1)} = \sum_{i=1}^{N} k_{zz}^i (h_i - h_{i-1}),$$

$$R_{kz}^{(2)} = \sum_{i=1}^{N} \int_{h_{j-1}}^{h_j} k_{zz}^j z dz,$$

$$R_{kx}^{(i)} = \sum_{i=1}^{N} \int_{h_{j-1}}^{h_j} k_{xx}^j z^{(i-1)} dz \quad i = 1,2,3,$$

$$R_c^{(i)} = \sum_{j=1}^{N} \int_{h_{j-1}}^{h_j} < \rho c_\nu >_j z^{(i-1)} dz \quad i = 1,2,3,$$

$$R_x^{(i)} = \sum_{j=1}^{N} \int_{h_{j-1}}^{h_j} < T_a \beta_{xx} >_j z^{(i-1)} dz \quad i = 1,2,3,$$

$$R_\theta^{(i)} = \sum_{j=1}^{N} \int_{h_{j-1}}^{h_j} < T_a \beta_{\theta\theta} >_j z^{(i-1)} dz \quad i = 1,2,3,$$

$$R_z^{(i)} = \sum_{j=1}^{N} \int_{h_{j-1}}^{h_j} < T_a \beta_{zz} >_j z^{(i-1)} dz \quad i = 1,2,3.$$

$$R_{x\theta}^{(i)} = \sum_{j=1}^{N} \int_{h_{j-1}}^{h_j} < T_a \beta_{x\theta} >_j z^{(i-1)} dz \quad i = 1,2,3.$$

The seven equations of motion (Equations 4), written in terms of the displacement and rotation components and the two energy Equations 11 and 12, constitute the governing equations for the nine dependent unknown functions u_0, v_0, w_0, ψ_θ, ψ_x, ψ_z, ϕ_z, T_0 and T_1. The governing equations are solved by means of the Galerkin finite element method, using initial and boundary conditions.

FINITE ELEMENT SOLUTION

Analytical solution of a cylindrical shell, with thermoelastic equilibrium Equations 4 and the coupled energy Equations 11 and 12, is practically not possible [1]. The finite element technique, based on the Galerkin method, is very efficient in solving coupled thermoelastic problems, including the coupled thermoelasticity of shells [3,5,7]. This method is used to obtain the solution of the coupled Equations 4, 11 and 12. The nodal degrees of a shell under axisymmetric load and coupled thermoelastic assumption are seven shell variables: u_0, v_0, w_0, ψ_θ, ψ_x, ψ_z, ϕ_z and two temperature variables: T_0 and T_1. A linear set of test functions are adopted to model the dependent functions [11]. Considering identical shape functions for all nine degrees of freedom and applying the formal Galerkin method to the system of seven shell equations and the two energy Equations 11 and 12 result in the following finite element equation.

$$[M]\{\ddot{d}\} + [C]\{\dot{d}\} + [K]\{d\} = \{F\}. \qquad (13)$$

The force matrix is divided into two terms, one term composed of the terms obtained through the weak formulation of the governing equations and the resulting natural boundary conditions and the second term, which include the components of external applied forces and thermal shocks. The process of the weak formulation and the terms which are selected for weak formulation in the governing equations are very important in regard to the resulting natural boundary conditions. The natural boundary conditions which are obtained as the result of the weak formulation should have either a kinematical meaning on the boundary or add up to make a traction boundary condition. Therefore, it is essential to set up possible kinematic and forced shell boundary conditions in advance and try to obtain them by the weak formulation [11].

The finite element equilibrium Equation 13 may be solved in the time domain by many techniques, such as Newmark, Houbolt, Wilson and other time integration techniques. In this paper, the α-method is used. According to this method, the equilibrium equation is transformed into the following form in the time domain [12].

$$[M]\{a\}_{n+1} + (1+\alpha)[C]\{v\}_{n+1} - \alpha[C]\{v\}_n + (1+\alpha)[K]\{d\}_{n+1} - \alpha[K]\{d\}_n = \{F(t_{n+\alpha})\}, \qquad (14)$$

where $t_{n+\alpha} = (1+\alpha)t_{n+1} - \alpha t_n = t_{n+1} + \alpha\triangle t$, $v = \dot{d}$ and $a = \ddot{d}$. The α-method become the Newmark methods when $\alpha = 0$. The displacement and velocity matrices at time step $(n+1)$ are written, in terms of their values

at time step n, as:

$$\{d\}_{n+1} = \{d\}_n + \Delta t\{v\}_n + \frac{\Delta t^2}{2}[(1-2\beta)\{a\}_n + 2\beta\{a\}_{n+1}], \quad (15)$$

$$\{v\}_{n+1} = \{v\}_n + \Delta t[(1-\gamma)\{a\}_n + \gamma\{a\}_{n+1}, \quad (16)$$

where γ and β are the accuracy and stability parameters, respectively. Using Equations 14 to 16, the unknown matrices $\{d\}_{n+1}$, $\{v\}_{n+1}$ and $\{a\}_{n+1}$ can be obtained in terms of their values at t_n.

The stability condition of the α-method, similar to methods such as Newmark, is based on positive definite matrices. Application of the Galerkin method to this problem results in nonaxisymmetric stiffness and damping matrices and, therefore, the resulting solution must be checked for its convergency. Selection of the time increment is important and has an absolute effect on solution convergency.

DISCUSSION AND RESULTS

Consider a multilayer thin cylindrical shell of thickness h, mean radius R and length L. The material constants of each individual layer are given in Table 1, where the definition of terms are given in the Nomenclature. The indices 1, 2, and n define the directions along the cylindrical shell axis, circumferential direction and thickness direction, respectively (see Figure 1). It is further assumed that the boundary conditions along the edges $x = 0$ and $x = L$ are clamped and zero initial conditions for displacements and velocities are considered. The thermal boundary conditions at the ends $x = 0$ and $x = L$ are assumed isolated, where the inside and outside surfaces transfer heat to the ambient by convection (with convective coefficients of h_i and h_o).

As the first example, a thin cylindrical shell of three orthotropic layers with ply angle stacking of [90/0/90] under pressure shock may be considered. The shell length, radius and thickness are assumed to be $L = 1$ m, $R = 0.15$ m, and $h = 0.015$ m, respectively. It is assumed that the inside pressure shock is uniformly applied by the following equation:

$$P_i(t) = 8 \times 10^6[1 - \exp(-1300t)]. \quad (17)$$

The inside pressure from Equation 17 reaches to a sustained maximum value of 8 Mpa within 0.4 msec. The shell is divided into 200 elements along the $x-$axis and time increment is selected as $\Delta t = 5 \times 10^{-6}$ sec. Shell behavior is studied up to the final time of 1 msec. Convergence of the finite element model used in this analysis, depends on the total number of elements, time increments and the numerical values of the stability coefficients α and β in the $\alpha-$method algorithm. The selected values of Δt and the total number of elements, along with the values of α and β, are all within the proper range of convergency.

Figure 2 shows the variation of the radial deflection of the shell middle plane at shell mid-length versus time for composite [90/0/90] and isotropic ($E = E_{11} =$ 196 Mpa) cylindrical shells. Due to the higher stiffness of the composite shell compared to the assumed isotropic shell, its lateral deflection is considerably smaller. The result compares well with the results of Noor and Burton [13]. Figure 3 is the plot of radial deflection versus the length of the shell for two different layer stackings [90/0/90] and [0/90/0]. The shell with layer stacking [90/0/90] has a higher stiffness and, thus, its deflection is lower. Although the energy equation is coupled with the shell thermoelastic equation, the temperature rise, due to the applied inside pressure, was found to be negligible and is not shown for this example. In addition to this result, it was found that for the assumed non-symmetric stacking sequence (three-layers composite), circumferential displacement is non-zero under axisymmetric loading.

The second example is a composite cylindrical shell with the material properties given in Table 1. The

Table 1. Material constants of each individual layer.

E_{11}	E_{22}	E_{1n}	G_{12}
196 GN/m^2	4.83 GN/m^2	4.83 GN/m^2	3.44 GN/m^2
G_{2n}	ν_{12}	ν_{2n}	k_{11}
3.44 GN/m^2	0.05	0.3	180 W/mk
k_{22}	k_{33}	α_{11}	α_{22}
67 W/mk	67 W/mk	$1.3 * 10^{-6}1/k$	$15 * 10^{-6}1/k$
α_{33}	h_i	h_o	
$15 * 10^{-6}1/k$	10000 W/m^2 k	200 W/m^2 k	

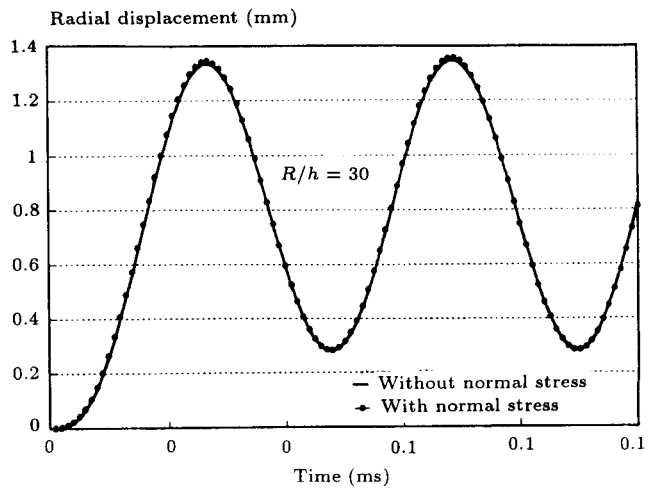

Figure 2. Radial deflection of cylindrical shell versus time under inside pressure shock.

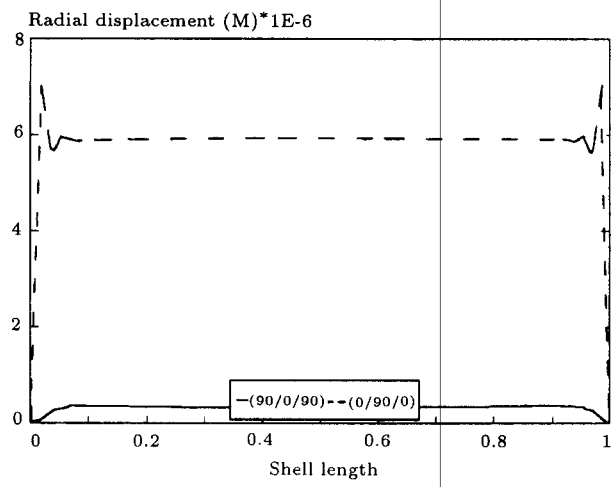

Figure 3. Effect of layer stacking of cylindrical shell under inside pressure shock.

mechanical and thermal boundary conditions are the same as in the first example. The shell is assumed to have three layers with stacking sequence [90/0/90] and is considered to be exposed to an inside temperature shock given by:

$$T_i(t) = 2207(1 - e^{-13100t}) + 293°\text{K}. \qquad (18)$$

The temperature of the inside surface rises rapidly from 293°K to 2500°K in 1 msec and the shell behavior is studied up to 4 sec. This time period of study is about 90 times larger than the time required for the thermal shock to reach its steady-state condition. The shell is divided into 100 elements along its length. The time increment is selected as $\Delta t = 10^{-5}$ sec and the $\alpha-$method stability coefficients are selected as $\alpha = 0.5$ and $\beta = 0.25$.

The inside temperature versus time is shown in Figure 4. The effect of thermo-mechanical coupling is shown in this figure. The curves in the time period $3 \leq t \leq 3.09$ are zoomed to show more clearly the difference between the coupled and uncoupled theories. For the uncoupled theory, the parameter β_{ij} in Equation 8 is set to zero and the energy equation is independently solved for T_0 and T_1. The results are then used in Equations 4 to obtain the thermoelastic response of the shell. It is observed from this figure that the coupled theory predicts slightly lower temperature distribution by time. This conclusion is validated by McQuillen and Brull [1] and is also in agreement with the results of Eslami et al. [5,7]. It is generally accepted that the coupled thermoelasticity theory predicts slightly lower temperature distribution in the structures [14].

In Figure 5 this comparison is shown for the middle plane radial deflection. It is noticed, that, while at $t = 0.45$ msec, the thermal shock reaches its steady state condition, the lateral deflection is still increasing. The reason is that the characteristic time of heat transfer is much larger than the mechanical characteristic time for stress wave. This behavior is different when the shell is under pressure shock [7]. In Figures 4 and 5, the values of temperature and displacement for a coupled condition is less than the values for an uncoupled condition. This means that the coupling effect acts like a damper and, thus, it could be regarded as thermoelastic damping. At the beginning of the shock, due to the lower values of strains, the difference between the coupled and uncoupled theories are negligible but, as time increases, the difference increases. This difference between the coupled and uncoupled solutions eventually vanishes for a large enough time, as expected. When temperature reaches its steady state condition, the strains reach their maximum values, while their time rate is decreased and the effect of mechanical coupling is increased. In Figures 6 and 7, the time history of axial force and moment at the inner surface is shown. Although both temperature and radial displacement are related

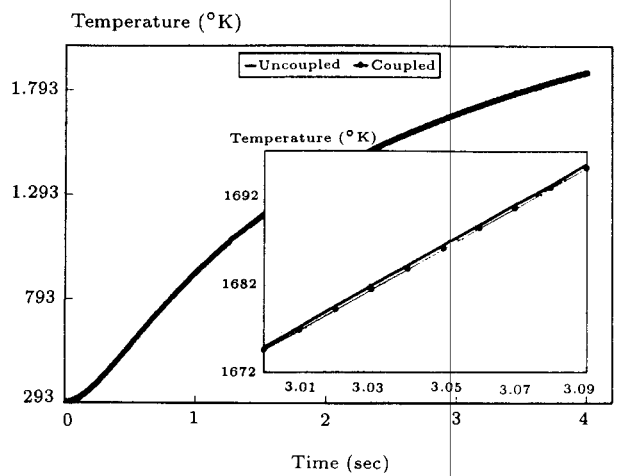

Figure 4. Effect of thermomechanical coupling on the temperature time history.

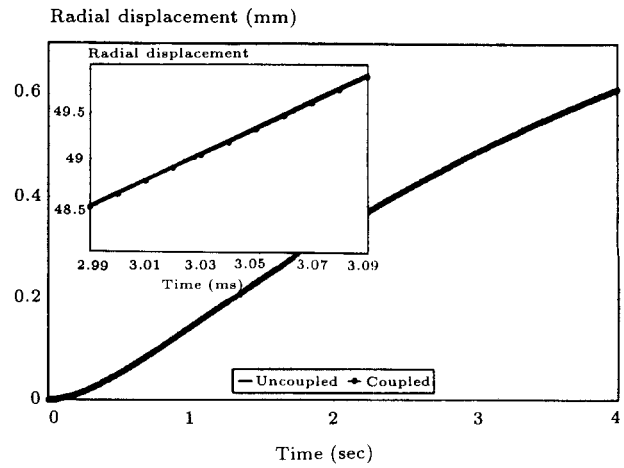

Figure 5. Effect of thermomechanical coupling on the radial displacement time history.

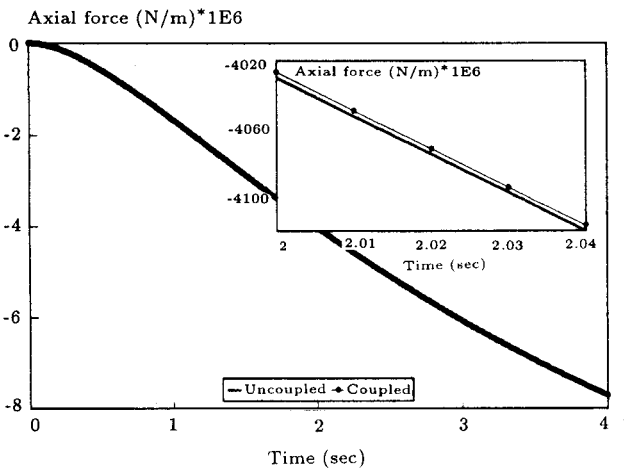

Figure 6. Effect of thermomechanical coupling on the axial force time history.

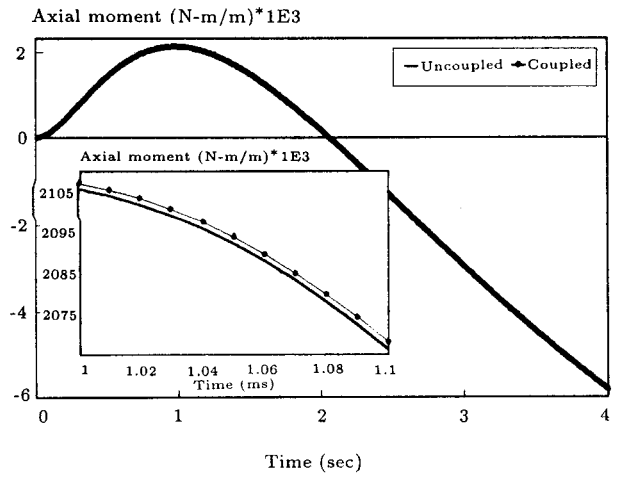

Figure 7. Effect of thermomechanical coupling on the axial moment time history.

to the axial force, due to their signs and magnitude, the effect of temperature is dominant and the axial force is negative. The variation of axial force and moment versus shell length are shown in Figures 8 and 9. As expected, ply angle will have an important effect on the response of a heated shell. The results are presented in Figures 10 and 11 for axial displacement versus length and axial stress versus thickness.

The effect of normal stress is studied in the next example. A simply supported cylindrical shell under uniform inside axisymmetric pressure and thermal shocks of:

$$P(t) = 8 * 10^6(1 - e^{-13100t}),$$

$$T_i(t) = 2207(1 - e^{-13100t}) + 293°\text{K}, \qquad (19)$$

is considered. Pressure reaches its maximum value at 1 msec. Figures 12 and 13 show the time history of the radial deflection in the middle length of the shell for two theories; when normal stress is considered (w is quadratic function of 2) and when normal stress is

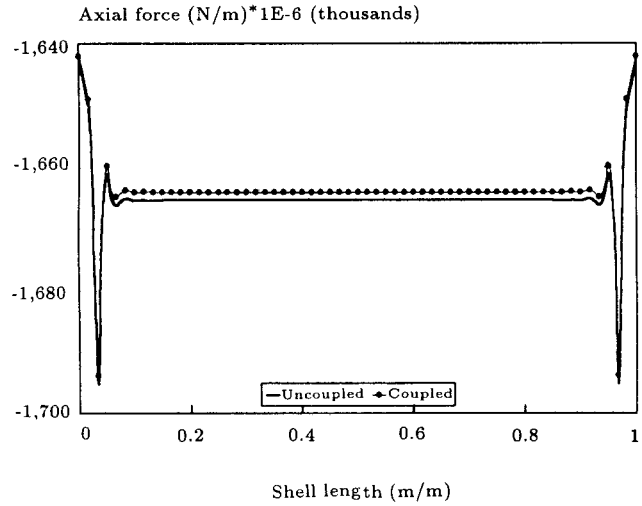

Figure 8. Effect of thermomechanical coupling on the axial force versus shell length.

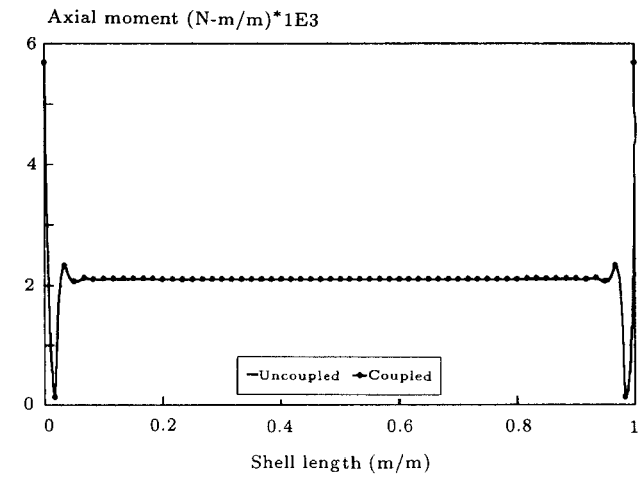

Figure 9. Effect of thermomechanical coupling on the axial moment versus the shell length.

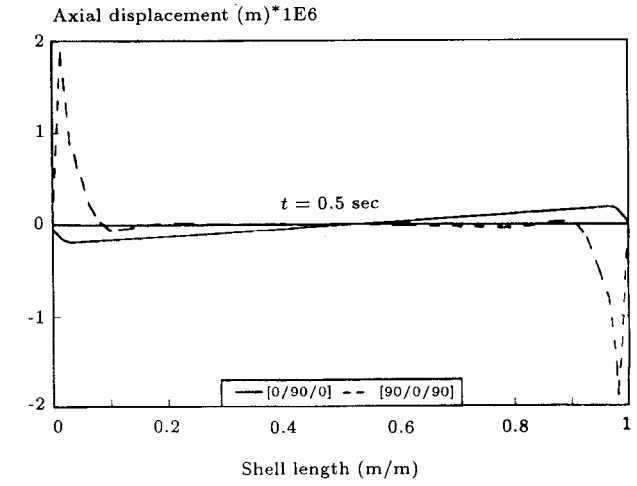

Figure 10. Effect of layer stacking on axial displacement in coupled theory.

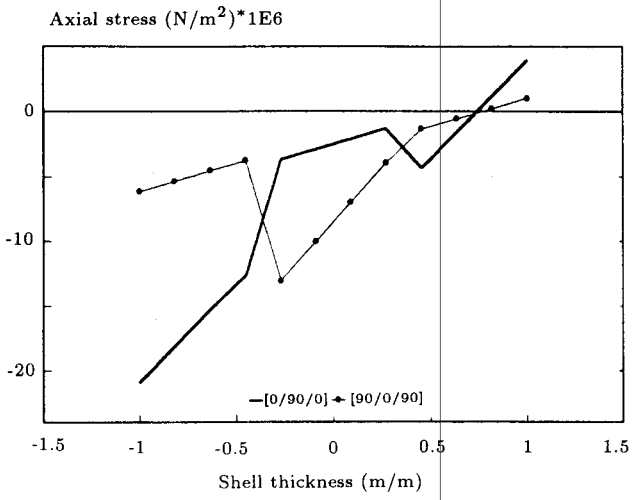

Figure 11. Effect of layer stacking on axial stress distribution through the thickness.

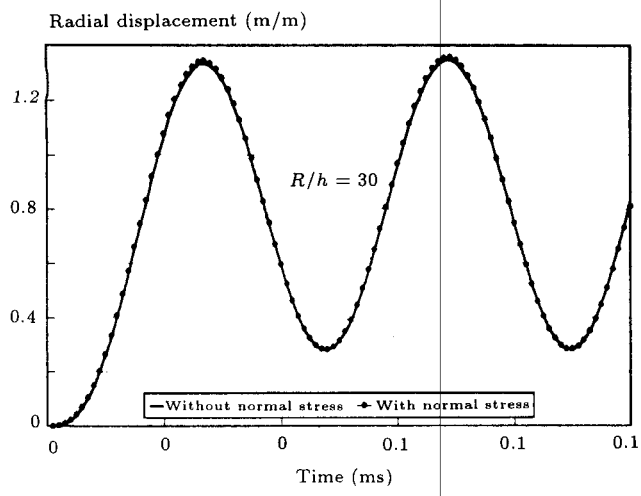

Figure 12. Time history of radial displacement at middle length of shell for two theories ($R/h = 30$).

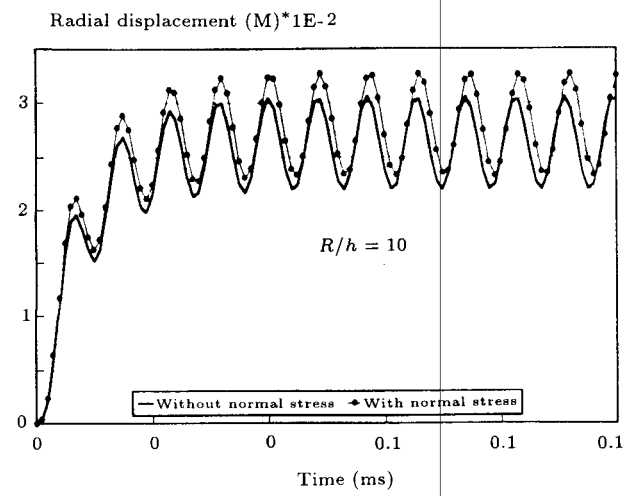

Figure 13. Time history of radial displacement at middle length of shell for two theories ($R/h = 10$).

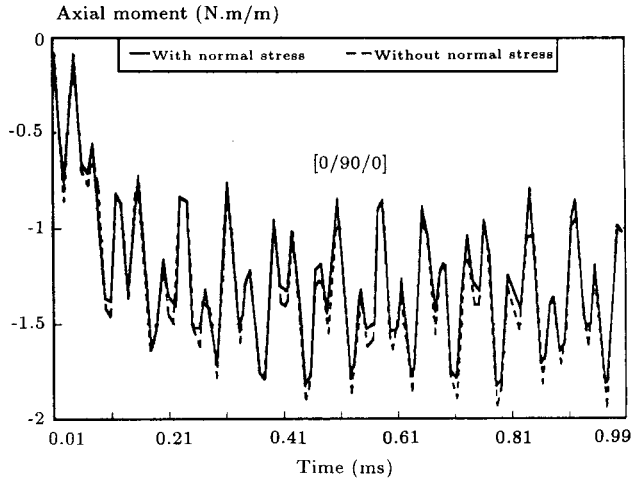

Figure 14. Time history of axial moment at middle length of shell for two theories ($R/h = 10$).

Table 2. Effect of normal stress (cylindrical shells).

Theories	w(m) ($R/H = 30$)	w(m) ($R/H = 10$)
Theory including σ_n	$3.1868E-4$	$5.0391E-5$
Theory excluding σ_n	$3.1417E-4$	$4.6686E-5$
Percent of difference	1.4	7.35

not considered (w is constant across the thickness) for $R/h = 30$ and $R/h = 10$, respectively. Table 2 gives the radial displacement for the middle length at 4.5 msec. The difference between the two cases is about 1.4% for $R/h = 30$ and 7.35% for $R/h = 10$.

In Figure 14, the time history of the axial moment at the middle length of the shell for $R/h = 30$ is plotted. It is observed that the effect of normal stress is to increase circumferential moment.

CONCLUSIONS

In this paper, a multilayered composite cylindrical shell under thermal and mechanical shock loads is considered. The fields of displacement and temperature are assumed to be coupled through a system of dynamic thermoelastic equations. The method of solution is based on the Galerkin finite element. Differences between the two theories, coupled and uncoupled, are presented for a thermal shock load. The coupled thermoelastic theory predicts lower values for temperature and displacement components, compared to the uncoupled theory. This conclusion is verified for structures and solution domains other than shells [3,14]. It is further concluded that the inclusion of normal stress and strain in the shell governing equations have a significant effect on the response of a shell under shock loads. This conclusion was also reached for shells of isotropic materials [7].

NOMENCLATURE

c_ν	specific heat at constant volume
E_{ij}	elastic moduli of individual layer
G_{ij}	shear moduli of individual layer
h	shell thickness
L	shell length
k_{ij}	conduction coefficients
$\bar{Q}_{ij}$	stiffness matrix
u_0, v_0, w_0	displacement components of the middle plane
R	cylinder mean radius
T_a	reference temperature
$\psi_x, \psi_\theta, \psi_z$	rotations
$\bar{\beta}_{ij}$	thermoelastic tensor
ϵ_{ij}	strain tensor
σ_{ij}	stress tensor
ν_{ij}	Poisson's ratios of individual layer
ρ	mass density

REFERENCES

1. McQuillen, E.J. and Brull, M.A. "Dynamic thermoelastic response of cylindrical shell", *Trans. ASME, J. Appl. Mech.*, pp 661-670 (1970).
2. Li, Y.Y., Ghoneim, H. and Chen, Y. "A numerical method in solving a coupled thermoelasticity equations and some results", *J. Thermal Stresses*, **9**, pp 345-358 (1986).
3. Eslami, M.R. and Vahedi, H. "A Galerkin finite element displacement formulation of coupled thermoelasticity spherical problems", *Trans. ASME, J. Press. Vess. Tech.*, **14**, pp 380-384 (1992).
4. Takazono, S., Tao, K. and Taguchi, T. "Elasto/ viscoplastic dynamic response of axisymmetric shells under mechanical and/or thermal loading", *Proc. ASME-PVP Conf.*, Hawaii (July 23-27 1989).
5. Eslami, M.R., Shakeri, M. and Sedaghati, R. "Coupled thermoelasticity of axially symmetric cylindrical shells", *J. Thermal Stresses*, **10**, pp 564-576 (1994).
6. Wang, X., Thangjitham, S. and Heller, R.A. "Response of a multilayered cylinder to thermal shock", *J. Thermal Stresses*, **14**, pp 47-64 (1991).
7. Eslami, M.R., Shakeri, M., Ohadi, A.R. and Shiari, B., "Coupled thermoelasticity of shells of revolution, effect of normal stress and coupling", *AIAA Journal*, **37**(4), pp 496-504 (1999).
8. Eslami, M.R., Shakeri, M. and Ohadi, A.R. "Coupled thermoelasticity of shells of revolution", *Proc. First Int. Symp. on Thermal Stresses*, Shizuoka University, Hamamatsu, Japan (1995).
9. Kraus, H., *Thin Elastic Shells* , John Wiley & Sons, Inc., New York, USA (1967).
10. Argris, J. and Tenek, L. "Recent advances in computational thermostructural analysis of composite plates and shells with strong nonlinearities", *Appl. Mech. Review*, **50**, pp 285-299 (1997).
11. Eslami, M.R. and Alizadeh, S.H. "Mixed Galerkin finite element analysis of non-axisymmetrically loaded spherical shells", *Scientica Iranica*, **1** (1994).
12. Bathe, K.J., *Finite Element Procedure in Engineering Analysis*, Prentice Hall Inc., New York, USA (1982).
13. Noor, A.K., and Burton, W.S. "Computational methods for high temperature multilayer composite plates and shells", *Appl. Mech. Rev.*, **45**, pp 419-446 (1992).
14. Chandrasekharalah, D.C. "Thermoelasticity with second sound: A review", *Appl. Mech. Rev.*, **39**, pp 355-375 (1986).

APPENDIX

$$\begin{bmatrix} N_x \\ N_\theta \\ A \\ N_{x\theta} \\ N_{\theta x} \\ M_x \\ M_\theta \\ B \\ M_{x,\theta} \\ M_{\theta x} \\ 2P_x \\ 2P_\theta \\ Q_\theta \\ S_\theta \\ S_x \\ 2T_\theta \\ 2T_x \end{bmatrix} = \begin{bmatrix} a_{11}^1 & a_{12} & a_{13}^2 & a_{16}^1 & a_{16} & b_{11}^1 & b_{12} & b_{13}^2 & b_{16}^1 \\ a_{12} & a_{22}^3 & a_{23}^4 & a_{26} & a_{26}^3 & b_{12} & b_{22}^3 & b_{23}^4 & b_{26} \\ a_{13}^2 & a_{23}^4 & a_{33}^5 & a_{36}^2 & a_{36}^4 & b_{13}^2 & b_{23}^4 & b_{33}^5 & b_{36}^2 \\ a_{16}^1 & a_{26} & a_{36}^2 & a_{66}^1 & a_{66} & b_{16}^1 & b_{26} & b_{36}^2 & b_{66}^1 \\ a_{16} & a_{26}^3 & a_{36}^4 & a_{66} & a_{66}^3 & b_{16} & b_{26}^3 & b_{36}^4 & b_{66} \\ b_{11}^1 & b_{12} & b_{13}^2 & b_{16}^1 & b_{16} & c_{11}^1 & c_{12} & c_{13}^2 & c_{16}^1 \\ b_{12} & b_{22}^3 & b_{23}^4 & b_{26} & b_{26}^3 & c_{11} & c_{22}^3 & c_{23}^4 & c_{26} \\ b_{13}^2 & b_{23}^4 & b_{33}^5 & b_{36}^2 & b_{36}^4 & c_{13}^2 & c_{23}^4 & c_{33}^5 & c_{36}^2 \\ b_{16}^1 & b_{26} & b_{36}^2 & b_{66}^1 & b_{66} & c_{16}^1 & c_{26} & c_{36}^2 & c_{66}^1 \\ b_{16} & b_{26}^3 & b_{36}^4 & b_{66} & b_{66}^3 & c_{16} & c_{26}^3 & c_{36}^4 & c_{66} \\ c_{11}^1 & c_{12} & c_{13}^2 & c_{16}^1 & c_{16} & d_{11}^1 & d_{12} & d_{13}^2 & d_{16}^1 \\ c_{12} & c_{22}^3 & c_{23}^4 & c_{26} & c_{26}^3 & d_{12} & d_{22}^3 & d_{23}^4 & d_{26} \\ 0 & 0 & 0 & 0 & 0 & 0 & 0 & 0 & 0 \\ 0 & 0 & 0 & 0 & 0 & 0 & 0 & 0 & 0 \\ 0 & 0 & 0 & 0 & 0 & 0 & 0 & 0 & 0 \\ 0 & 0 & 0 & 0 & 0 & 0 & 0 & 0 & 0 \\ 0 & 0 & 0 & 0 & 0 & 0 & 0 & 0 & 0 \\ 0 & 0 & 0 & 0 & 0 & 0 & 0 & 0 & 0 \end{bmatrix}$$

$$\begin{bmatrix} b_{16} & c_{11}^1 & c_{12} & 0 & 0 & 0 & 0 & 0 & 0 \\ b_{26}^3 & c_{12} & c_{22}^3 & 0 & 0 & 0 & 0 & 0 & 0 \\ b_{36}^4 & c_{13}^2 & c_{23}^4 & 0 & 0 & 0 & 0 & 0 & 0 \\ b_{66} & c_{16}^1 & c_{26} & 0 & 0 & 0 & 0 & 0 & 0 \\ b_{66}^3 & c_{16} & c_{26}^3 & 0 & 0 & 0 & 0 & 0 & 0 \\ c_{16} & d_{11} & d_{12} & 0 & 0 & 0 & 0 & 0 & 0 \\ c_{26}^3 & d_{12} & d_{22}^3 & 0 & 0 & 0 & 0 & 0 & 0 \\ c_{36}^4 & d_{13}^2 & d_{23}^4 & 0 & 0 & 0 & 0 & 0 & 0 \\ c_{66} & d_{16}^1 & d_{26} & 0 & 0 & 0 & 0 & 0 & 0 \\ c_{66}^3 & d_{16} & d_{26}^3 & 0 & 0 & 0 & 0 & 0 & 0 \\ d_{16} & e_{11}^1 & e_{12} & 0 & 0 & 0 & 0 & 0 & 0 \\ d_{26}^3 & e_{12} & e_{22}^3 & 0 & 0 & 0 & 0 & 0 & 0 \\ 0 & 0 & 0 & a_{44}^3 & a_{45} & b_{44}^3 & b_{45} & c_{44}^3 & c_{45} \\ 0 & 0 & 0 & a_{45} & a_{55}^1 & b_{45} & b_{55}^1 & c_{45} & c_{55}^1 \\ 0 & 0 & 0 & b_{44}^3 & b_{45} & c_{44}^3 & c_{45} & d_{44}^3 & d_{45} \\ 0 & 0 & 0 & b_{45} & b_{55}^1 & c_{45} & c_{55}^1 & d_{45} & d_{55}^1 \\ 0 & 0 & 0 & c_{44}^3 & c_{45} & d_{44}^3 & d_{45} & e_{44}^3 & e_{45} \\ 0 & 0 & 0 & c_{45} & c_{55}^1 & d_{45} & d_{55}^1 & e_{45} & e_{55}^1 \end{bmatrix}$$

$$\begin{bmatrix} \epsilon_1^0 \\ \epsilon_2^0 \\ w_1 \\ \beta_1^0 \\ \beta_2^0 \\ \epsilon_1' \\ \epsilon_2' \\ w_2 \\ \beta_1' \\ \beta_2' \\ \frac{1}{2}\epsilon_{1,\prime} \\ \frac{1}{2}\epsilon_{2,\prime} \\ \mu_2^0 \\ \mu_1^0 \\ \mu_2' \\ \mu_{1,\prime} \\ \frac{1}{2}\mu_{2,\prime} \\ \frac{1}{2}\mu_1 \end{bmatrix} = \begin{bmatrix} at_2^2 & bt_1^2 \\ at_1^4 & bt_2^4 \\ at_2^5 & bt_1^5 \\ at_{12}^2 & bt_{12}^2 \\ at_{12}^4 & bt_{12}^4 \\ bt_2^2 & ct_1^2 \\ bt_1^4 & ct_2^4 \\ bt_2^5 & ct_1^5 \\ bt_{12}^2 & ct_{12}^2 \\ bt_{12}^4 & ct_{12}^4 \\ ct_2^1 & dt_1^2 \\ ct_1^4 & dt_2^4 \\ 0 & 0 \\ 0 & 0 \\ 0 & 0 \\ 0 & 0 \\ 0 & 0 \end{bmatrix} \begin{bmatrix} T_0 \\ T_1 \end{bmatrix}$$

where $a_{ij}^m, b_{ij}^m, c_{ij}^m, d_{ij}^m, e_{ij}^m$ are:

$$(a_{ij}, b_{ij}, c_{ij}, d_{ij}, e_{ij}) =$$

$$(a_{ij}^4, b_{ij}^4, c_{ij}^4, d_{ij}^4, e_{ij}^4) =$$

$$(\bar{Q}_{ij})_k \sum_{k=1}^{N} \int_{h_{k-1}}^{h_k} (1, z, z^2, z^3, z^4) dz,$$

$$(a_{ij}^1, b_{ij}^1, c_{ij}^1, d_{ij}^1, e_{ij}^1) =$$

$$(a_{ij}^2, b_{ij}^2, c_{ij}^2, d_{ij}^2, e_{ij}^2) =$$

$$(a_{ij}^5, b_{ij}^5, c_{ij}^5) =$$

$$(\bar{Q}_{ij})_k \sum_{k=1}^{N} \int_{h_{k-1}}^{h_k} (1, z, z^2, z^3, z^4) dz,$$

$$(a_{ij}^3, b_{ij}^3, c_{ij}^3, d_{ij}^3, e_{ij}^3) =$$

$$(\bar{Q}_{ij})_k \sum_{k=1}^{N} \int_{h_{k-1}}^{h_k} \frac{1}{(1 + z/R)} (1, z, z^2, z^3, z^4) dz,$$

$$(at_i, bt_i, ct_i, dt_i) = (at_i^2, bt_i^2, ct_i^2, dt_i^2) =$$

$$(\bar{\beta}_i)_k \sum_{k=1}^{N} \int_{h_{k-1}}^{h_k} \frac{1}{1 + z/R} (1, z, z^2, z^3) dz,$$

$$(at_i^1, bt_i^1, c_i^1, d_i^1) =$$

$$(\bar{\beta}_i)_k \sum_{k=1}^{N} \int_{h_{k-1}}^{h_k} (1, z, z^2, z^3) dz,$$

$$\epsilon_x^0 = u_{o,x}, \epsilon_\theta^0 = \frac{v_{o,\theta}}{R} + \frac{w_o}{R}, \epsilon_x' = \psi_{x,x}, \epsilon_\theta' = \frac{\psi_{\theta,\theta}}{R} + \frac{\psi_z}{R},$$

$$\epsilon_x'' = 0, \epsilon_\theta' = \frac{\phi_z}{R}, \beta_x^0 = v_{o,x},$$

$$\beta_\theta^0 = u_{o,\theta} R,$$

$$\beta_x' = \psi_{\theta,x}, \beta_\theta' = \psi_{x,\theta},$$

$$\mu_x^0 = w_{o,x} + \psi_x, \mu_\theta^0 = \frac{w_{o,\theta} - v_o}{R} + \psi_\theta,$$

$$\mu_x' = \psi_{z,x}, \mu_\theta' = \frac{\psi_{z,\theta}}{R}, \mu_x'' = \phi_{z,x}, \mu_\theta'' = \frac{\psi_{z,\theta}}{R}$$